

Residual Carbon Evolution in BaTiO₃ Ceramics Studied by XPS after Ion Etching

C. Miot,^a E. Husson,^{a*} C. Proust,^a R. Erre^b and J. P. Coutures^a

^aCRPHT, CNRS UPR 4212, 45071 Orléans cedex 2, France

^bCRMD, CNRS et Université d'Orléans 45071 Orléans cedex 2, France

(Received 17 March 1997; revised version received 4 June 1997; accepted 16 June 1997)

Abstract

The surface of BaTiO₃ ceramics and a freshly fractured ceramic surface were studied by X-ray photoelectron spectroscopy (XPS). Ti_{2p}, Ba_{3d}, O_{1s} and C_{1s} photopeaks were analysed before and after Ar⁺ ion sputter etching. Then the evolution of the Ba_{3d} and C_{1s} spectra after a long bombardment at liquid nitrogen temperature was recorded as a function of time and during reheating to room temperature. The intrinsic residual carbon of the material was found to occur in the form of C–O groups and low energy C* carbon at binding energies of 287 and 282 eV, respectively. © 1998 Elsevier Science Limited.

Resumé

La surface et la fracture de céramiques de BaTiO₃ ont été étudiées par spectroscopie de photoélectrons. Les spectres des niveaux Ti_{2p}, Ba_{3d}, O_{1s} et C_{1s} sont analysés avant et après un décapage par bombardement d'ions Ar⁺. Puis l'évolution des spectres des niveaux Ba_{3d} et C_{1s} après un long bombardement ionique à la température de l'azote liquide est suivie en fonction du temps et lors du réchauffement jusqu'à 20°C. Le carbone résiduel intrinsèque au matériau est mis en évidence et détecté sous forme de groupes C–O et de carbone de basse énergie, respectivement, à 287 et 282 eV.

1 Introduction

The use of organic precursors in the preparation of homogeneous, fine powders to obtain ceramic materials of improved properties, is still extensively researched. This type of process may leave residual carbon in powders and even in ceramics after the

sintering step. Very little has been published on the subject.¹ In the eighties, Freund and his co-workers^{2–5} studied the carbon present in several single crystals of both natural and synthetic oxides such as magnesium oxide, olivine or forsterite. They used predominantly the (d,p) nuclear method; only one paper³ reports on an X-ray photoelectron spectroscopy (XPS) analysis. No study on ceramic oxides has been found in the literature to date.

XPS gives information on the chemical form of carbon in the surface layer of 10–15 Å.³ By ion etching, it is possible to remove several layers of atoms and thus contaminants on the surface. After this process, the intrinsic carbon of the material can be determined. In a previous paper,⁶ we analysed the C_{1s}, O_{1s}, Ti_{2p}, Ba_{3d} and Ba_{4d} photoelectron peaks of powder and ceramics of BaTiO₃. In this paper, we present the evolution of the photoelectron peaks and more particularly the C_{1s} signal as a function of time after ion-etching of a ceramic surface (hereafter called 'surface') and of a freshly fractured ceramic surface (hereafter called 'fracture').

2 Experimental

2.1 Sample preparation

BaTiO₃ powders were obtained from a citric resin method described in previous papers.^{7,8} The mixed citrate BaTi(C₆H₆O₇)₃·6H₂O was first prepared, then dissolved in a mixture of citric acid, ethylene glycol and water. The ratio R = (BaTiO₃ mass)/(solution mass) was 1%. This mixture was calcined at 700°C in static air and BaTiO₃ powders were obtained after 2 h. Powders prepared by this method exhibited a Ba/Ti ratio equal to 1. After a careful deagglomeration step,⁸ the powders were annealed again at 700°C for 4 h before being pressed at 250 MPa into discs and then sintered. The following sintering cycle was used: 20–700°C at

*To whom correspondence should be addressed.

350° h⁻¹; 700–1000°C at 50° h⁻¹ and 1000–1230°C at 4° h⁻¹. The ceramics obtained exhibited an average grain size of 1.6 μm, and a density equal to 96% of the theoretical density, thus good dielectric properties were obtained.⁹

2.2 XPS spectra

XPS spectra were recorded with an Escalab MK2 (Vacuum Generator System) using Mg K_α radiation. As the technique is sensitive to the composition of only a few atomic layers, it requires ultrahigh

vacuum (UHV) conditions to avoid or minimize surface contamination. Residual pressure in the analysis chamber was about 10⁻⁹ mbar. Spectra were calibrated using the adventitious carbon fixed at binding energy (B.E.) of 284.6 eV to compensate the charge effects. The photoelectron peaks were numerically fitted using Lorentzian-Gaussian mixed functions after an integral background subtraction. Ar⁺ ion etching was performed at 5 keV during variable periods of time. A sample holder at liquid nitrogen temperature allowed the

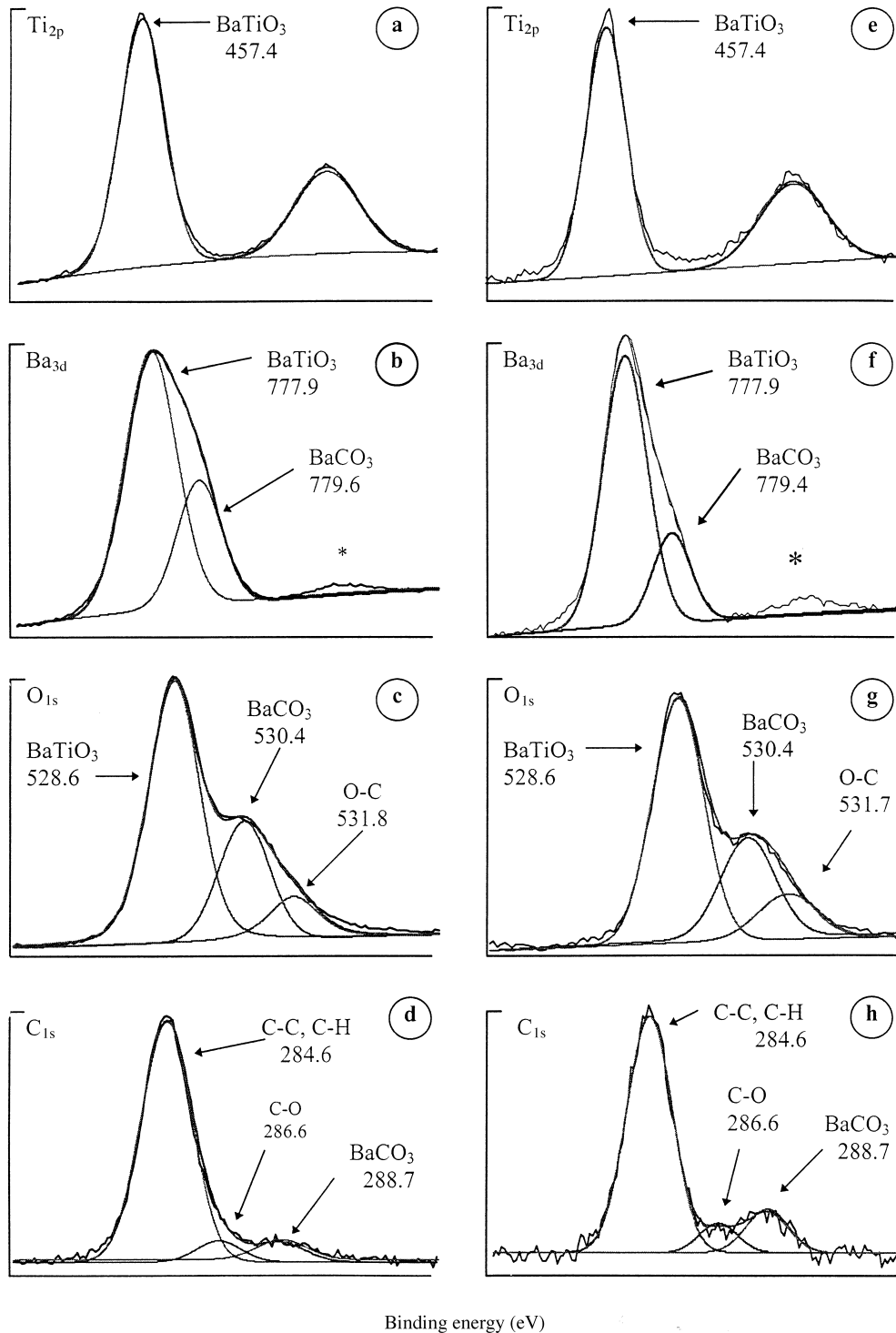


Fig. 1. XPS normalised spectra of a surface of a BaTiO₃ ceramic: (a) Ti_{2p}, (b) Ba_{3d}, (c) O_{1s}, (d) C_{1s} signals and of a freshly fractured ceramic surface (e) Ti_{2p}, (f) Ba_{3d}, (g) O_{1s}, (h) C_{1s} signals. * Extra line.

samples to be cooled during etching. After the ion etching, spectra were recorded hour after hour at liquid nitrogen temperature for about 7 h, and for several hours again after the cooling system had been switched off. The sample temperature increased up to the room temperature in about one hour. After the ion etching, spectra were calibrated using the signal of the heaviest and thus the least perturbed atom, i.e. Ba_{3d} level fixed at 777.9 eV.

3 Results and Discussion

3.1 XPS spectra of a BaTiO₃ ceramic surface and a fresh fracture before ion-etching

Figure 1(a)–(d) gives the Ti_{2p}, Ba_{3d}, O_{1s}, and C_{1s} photoelectron peaks of the surface of a just sintered ceramic. The Ti_{2p} photoelectron peak reveals only titanium in BaTiO₃. The Ba_{3d} signal exhibits two components at 777.9 eV (I~66%) and 779.6 eV (I~34%) with FWHM (full width at half maximum) 2eV corresponding to barium in BaTiO₃ and in BaCO₃, respectively. The O_{1s} signal displays three components with FWHM 1.75 eV at 528.6 eV (I~66%), 530.4 eV (I~26%) and 531.8 eV (I~8%) assigned to oxygen in BaTiO₃, CO₃²⁻ ions and C–O groups, respectively. The C_{1s} peak displays also three contributions with FWHM of 2 eV: the main peak (I~70% of the signal intensity) at 284.6 eV corresponds to the C–C/C–H groups; the second and third peaks at 288.7 eV (I~20%) and 286.6 eV (I~10%) have been assigned to CO₃²⁻ ions and C–O groups, respectively, in accordance with the O_{1s} signal assignment.

Figure 1(e)–(h) displays the photoelectron peaks obtained with the fractured surface of a ceramic, the ceramic being fractured just before the sample was introduced into the UHV chamber. The Ba_{3d} peak [Fig. 1(f)] shows a less pronounced contribution of BaCO₃ than that found at the surface [Fig. 1(b)], which is confirmed by the O_{1s} peak profile [Fig. 1(g)]. For the C_{1s} peak [Fig. 1(h)] the BaCO₃ contribution is relatively more important as against the C–C/C–H peak comparing the surface and the fracture [Fig. 1(d)]. The BaCO₃ and C–C/C–H contributions observed in the fracture spectra are due to contamination occurring in the interval of time between the fracturing of the surface and the introduction of the sample into the UHV chamber. The contribution of the C–O groups on the contrary, is practically constant in the fracture and surface O_{1s} and C_{1s} photoelectron peaks.

3.2 Evolution of XPS spectra after ion-etching

After an ion etching of 180 s, XPS spectra of the surface and the fracture show that the contributions

of the CO₃²⁻ and C–C/C–H groups have practically disappeared. Therefore these species can only be located at the surface of the ceramic in a layer of 10–20 Å depth. The C_{1s} spectrum of the surface (Fig. 2) exhibits two small peaks at 287.3 eV and 282 eV assigned to C–O groups and a low-energy carbon species called C*, respectively.⁶ No peak appears in the C_{1s} spectrum of the fracture.

After obtaining these first results, we then studied the evolution of XPS spectra of a ceramic surface as a function of time after an ion etching of 30 min at liquid nitrogen temperature. Figure 3 shows the evolution of the Ba_{3d} peak. Immediately after the ion etching, the peak is very large (FWHM # 5.5 eV) which can be referred to a disordered state due to the interaction between Ar⁺ ions and BaTiO₃ material. A weak evolution is observed until cooling stops. Then, the peak sharpens and its profile remains practically constant over time. Heating removes local disorder in the material. The final FWHM is about 2 eV as in the spectrum of the freshly sintered ceramic. The Ba_{4d}, Ti_{2p} and O_{1s} peaks exhibit the same behaviour. Figure 4(a) shows the evolution of the C_{1s} signal under the same conditions. Two large and weak peaks progressively appear at 287 and 282 eV assigned to C–O groups and C* carbon, respectively. After the cooling switch cut off, the two

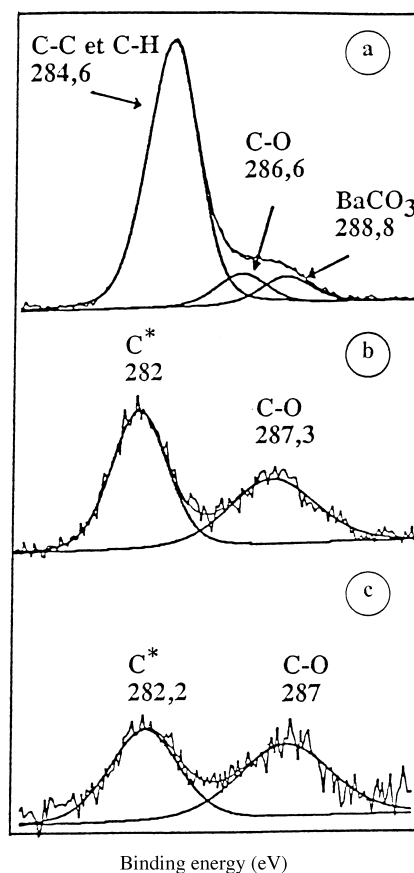


Fig. 2. C_{1s} XPS spectra of a surface of a BaTiO₃ ceramic: (a) before and after (b) one and (c) three Ar⁺ ion etching of 180 s.

peaks sharpen. The C–O peak remains quite constant whereas the intensity of the C* peak increases continuously as a function of time for several hours. The presence of C–O groups is confirmed by a contribution to the O_{1s} peak at 532 eV BE. This result shows the mobility of the two carbon species, particularly that of C* carbon.

The same experiment was performed with a fractured ceramic. Figure 4(b) displays the evolution of the C_{1s} peak as a function of time. After the ion etching no species is detected. Then two peaks appear at 287 and 282 eV, the first exhibiting the larger contribution. At the end of cooling, the C–O peak is almost unchanged whereas the intensity of the C* peak gradually increases for several hours. Again the mobility of the two carbon species is shown.

Comparison of the C_{1s} peaks given in Fig. 4(a) and (b) shows that the contribution of the C–O groups is smaller in the fracture than in the surface. This observation agrees with previous results;¹⁰ the ¹²C(d,p)¹³C nuclear technique measurements revealed the existence of a gradient of C concentration from the 0.4 μm depth surface layer (several hundreds ppm) to the bulk (about 50 ppm); moreover, we showed¹¹ that during the sintering step, residual carbon present in the powder diffuses from the bulk to the surface of the ceramic. The C–O groups detected may correspond to the C–O⁻ groups

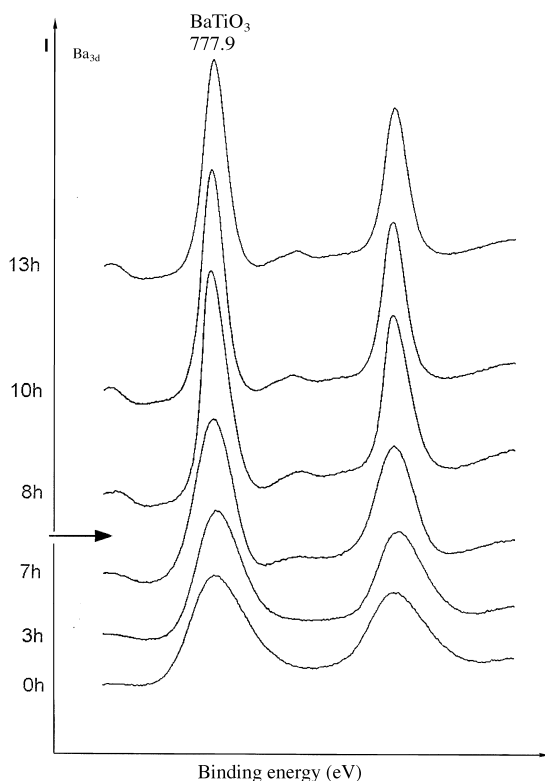


Fig. 3. Evolution of the Ba_{3d} XPS spectrum of a surface of a BaTiO₃ ceramic as a function of time (in h) after 30 min ion-etching at liquid nitrogen temperature. Arrow indicates the end of cooling time. * Extra line.

described by Freund *et al.* in MgO single crystals.⁴ According to these authors, the carbon diffusion proceeds by successive formation of C–O⁻ bonds when highly mobile atomic carbon moves through the oxygen lattice. Atomic carbon should occupy vacant cationic sites or tetrahedral interstices of the fcc structure of MgO.

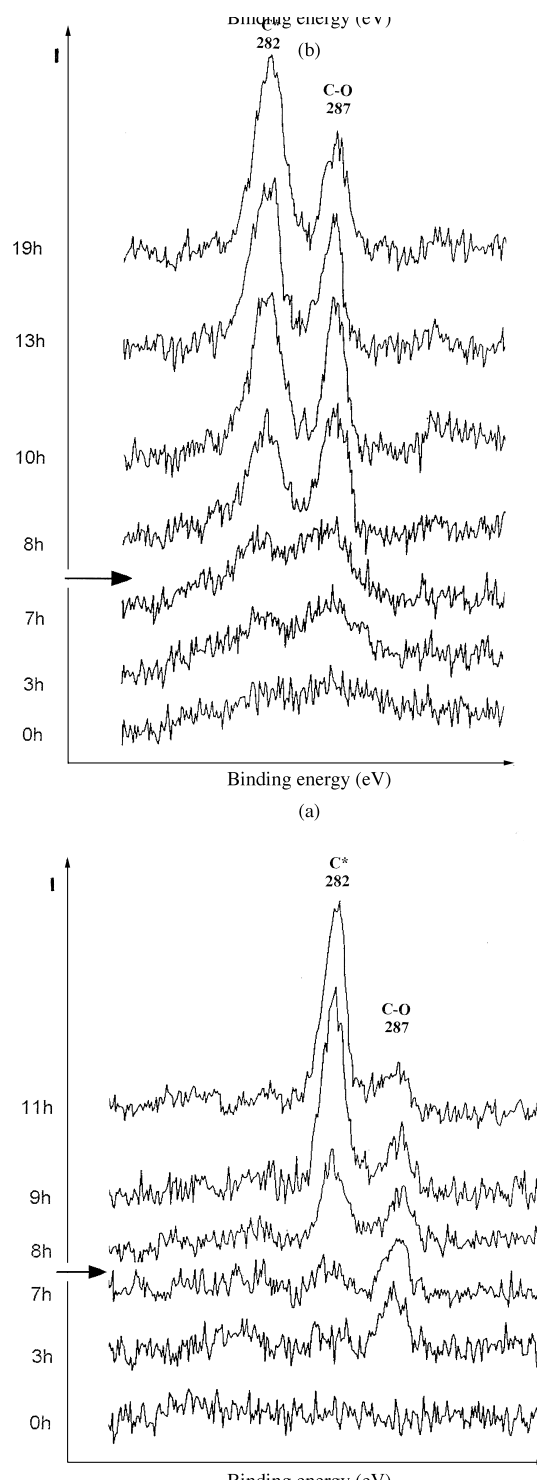


Fig. 4. Evolution of the C_{1s} XPS spectrum of a BaTiO₃ ceramic as a function of time (in h) after 30 min ion-etching at liquid nitrogen temperature. Arrows indicate the end of cooling time. (a) Ceramic surface, (b) freshly fractured ceramic surface.

The low energy carbon component (about 282 eV BE) exhibits a binding energy close to that of carbides;^{12–15} for example the B.E. of C in TiC is observed to be between 281.5 and 282 eV.^{12,13,15} Johansson *et al.*¹⁶ studying the TiC crystal surface observed a main component in the C_{1s} signal at 281.5 eV interpreted as originating from carbon in carbide and a fairly weak component at 282 eV assigned to carbon segregated at the TiC surface after Ar⁺ ion sputtering and repeated flash heating. Its intensity increased when the TiC crystal was flash heated to higher temperatures. In our case, the presence of TiC is very unlikely; moreover, we have not detected in the Ti_{2p} signal a component at 455 eV¹⁵ corresponding to Ti in TiC. The C* species originates from intrinsic carbon and exhibits a high mobility.

4 Conclusion

This study shows the XPS spectra of surface and fracture of BaTiO₃ ceramics obtained by the citric route before and after Ar⁺ ion-etching. The C–C/C–H groups detected are essentially due to atmospheric contamination and are located only in the first surface atomic layers of the material since they disappeared after the first ion etching. The same observation is made for the CO₃^{2–} groups: thus it can be stated that the method used for the powder synthesis gives a material with a very low content of free barium^{7,8} that the XPS can detect. On the contrary, the C–O groups, present before and after ion etching are material intrinsic. The low energy carbon C* is detected at 282 eV only after ion-etching. It corresponds also to a material intrinsic carbon species.

Acknowledgement

The authors are indebted to R. Benoit for recording XPS spectra.

References

1. Barboux, P., Griesmar, P., Ribot, F. and Mazerolles, L., Homogeneity-related problems in solution derived powders. *J. of Solid State Chem*, 1995, **117**, 343–350.
2. Wengeler, H., Knobel, R., Kathrein, H., Freund, F., Demortier, G. and Wolff, G., Atomic carbon in magnesium oxide single crystals. Depth profiling, temperature- and time-dependent behavior. *J. Phys. Chem. Solids*, 1982, **43**, 59–71.
3. Oberheuser, G., Kathrein, H., Demortier, G., Gonska, H. and Freund, F., Carbon in olivine single crystals analyzed by the ¹²C(d,p)¹³C method and by photoelectron spectroscopy. *Geochimica and Cosmochimica Acta*, 1983, **47**, 1117–1129.
4. Freund, F., Wengeler, H., Kathrein, H., Knobel, R., Oberheuser, G., Maiti, G. C., Reil, D., Knipping, U. and Kotz, J., Hydrogen and carbon derived from dissolved H₂O and CO₂ in minerals and melts. *Bull. Mineral*, 1983, **106**, 185–200.
5. Freund, F., Presence, segregation and reactivity of H, C and N dissolved in some refractory oxides. *J. de Physique Colloque C1*, 1986, **47**, 499–508.
6. Miot, C., Husson, E., Proust, C., Erre, R. and Coutures, J. P., XPS characterization of barium titanate ceramics prepared by the citric route. Residual carbon study. *J. of Mater. Res*, 1997, **17**, 2388–2392.
7. Coutures, J. P., Odier, P. and Proust, C., Barium titanate formation by organic resins formed with mixed citrate. *J. Mater. Sci.*, 1992, **27**, 1849–1856.
8. Proust, C., Miot, C. and Husson, E., Characterization of BaTiO₃ powder obtained by a chemical route. *J. Europ. Ceram. Soc.*, 1995, **15**, 631–635.
9. Miot, C., Proust, C. and Husson, E., Dense ceramics of BaTiO₃ produced from powders prepared by a chemical process. *J. Europ. Ceram. Soc.*, 1995, **15**, 1163–1170.
10. Miot, C., Proust, C., Husson, E., Blondiaux, G. and Coutures, J. P., Ageing influence on residual carbon content in different grain sized BaTiO₃ analysed ceramics by ¹²C(d,p)¹³C nuclear method. *J. of Europ. Ceram. Soc.*, 1997, **17**, 1335–1340.
11. Proust, C., Husson, E., Blondiaux, G. and Coutures, J. P., Residual carbon detection in barium titanate ceramics by nuclear reaction technique. *J. of Europ. Ceram. Soc.*, 1994, **14**, 215–219.
12. Jouan, P. Y., Peignon, M. C., Cardinaud, C. H. and Lempérière, G., Characterization of TiN coatings and of the TiN/Si interface by X-ray photoelectron spectroscopy and Auger electron spectroscopy. *Applied Surf. Science*, 1993, **68**, 595–603.
13. Ramqvist, L., Hamrin, K., Johansson, G., Fahlman, A. and Nordling, C., Charge transfer in transition metal carbides and related compounds studied by ESCA. *J. Phys. Chem. Solids*, 1969, **30**, 1835–1847.
14. O'Keefe, M. J., Horiuchi, S., Rigsbee, J. M. and Chu, J. P., Effect of oxygen and carbon on the formation and stability of A-15 crystal structure chromium thin films. *Thin Solid Films*, 1994, **247**, 169–177.
15. Bertocello, R., Casagrande, A., Casarin, M., Glisenti, A., Lanzoni, E., Mirengi, L. and Tondello, E., TiN, TiC and Ti(C,N) film characterization and its relationship to tribological behaviour. *Surface and Interface Analysis*, 1992, **18**, 525–531.
16. Johansson, L. I., Johansson, H. I. P. and Hakansson, K. L., Surface-shifted N 1s and C 1s levels on the (100) surface of TiN and TiC. *Phys. Rev. B*, 1993, **48**, 14520–14523.